

Electronic structure and lifetime broadening of a quantum-well state on $p(2 \times 2)$ K/Cu(111)S. Achilli,¹ G. Butti,¹ M. I. Trioni,² and E. V. Chulkov^{3,4}¹*Dipartimento di Scienza dei Materiali, Università di Milano-Bicocca, Via Cozzi 53, 20125 Milano, Italy*²*CNISM and CNR-INFM, UdR Milano-Bicocca, via Cozzi 53, 20125 Milano, Italy*³*Donostia International Physics Center (DIPC), P. de Manuel Lardizabal 4, San Sebastián, 20018 Basque Country, Spain*⁴*Departamento de Física de Materiales, Facultad de Ciencias Químicas, UPV/EHU and Centro de Física de Materiales (CFM) (CSIC-UPV/EHU), Apdo. 1072, San Sebastián, 20080 Basque Country, Spain*

(Received 21 August 2009; revised manuscript received 8 October 2009; published 23 November 2009)

We studied a quantum-well state (QWS) generated by the adsorption of one monolayer of K on Cu(111) surface by means of a first principles approach. We calculated the electronic properties of the system within the Inglesfield's embedding method, which enables us to investigate the elastic linewidth of surface states. Our findings are in good agreement with recent experimental results obtained from photoemission spectroscopy measurements for binding energy and \mathbf{k}_{\parallel} dispersion. We also studied the contributions to the QWS linewidth due to electron-electron many-body effects and electron-phonon scattering in Hedin's *GW* approach and within the Debye model, respectively. The main contribution to the linewidth is due to intraband transitions within the QWS itself, accounting for ~ 16 meV to the total width. The elastic, electron-phonon, and interband transition contributions are smaller than 3 meV each.

DOI: [10.1103/PhysRevB.80.195419](https://doi.org/10.1103/PhysRevB.80.195419)

PACS number(s): 73.20.At, 73.21.Fg, 73.61.At

I. INTRODUCTION

Since 1935,¹ the chemisorption of single alkali atoms on metal surfaces has extensively been explored both experimentally^{2–6} and theoretically.^{7–14} Not only electron levels, but also the lifetimes of excited electrons have been studied. As the alkali coverage increases, the wave functions of the adatoms start to overlap and the electron levels turn into dispersing bands, the so-called quantum-well states (QWSs), which differ greatly in energy from the original levels of the adsorbed single adatoms. Such QWSs have been studied in alkali overlayers on noble metals, aluminum, and other metal surfaces.^{15–27} The most studied systems of alkali coverages are $p(2 \times 2)$ structures of Na, K, and Cs on Cu(111). This structure is the saturation monolayer for K and Cs, while it is a submonolayer coverage for the Na overlayer. Experiments show that the QWS in $p(2 \times 2)$ Na/Cu(111) and Cs/Cu(111) is located just above the Fermi level (E_F), at 408 and 42 meV, respectively,²⁸ while in the K/Cu(111) system such a state is located just below E_F , at $E = -80 \pm 30$ meV²⁹ and $E = -110$ meV.³⁰ *Ab initio* calculations performed for Na/Cu(111) and Cs/Cu(111) have confirmed the unoccupied position of QWS.^{28,31} Corriol *et al.*²⁸ also performed a theoretical analysis of the decay mechanisms for excited electrons in QWS and found that for both systems, in contrast to the full monolayer of Na on Cu(111), which is characterized by a $(3/2 \times 3/2)$ reconstruction,³² the many-body inelastic electron-electron ($e-e$) scattering contribution to the lifetime broadening is negligibly small and the broadening is equally determined by one-electron energy conserving process and electron-phonon (e -ph) interaction.

In this work, we present an embedding method electronic structure study of the $p(2 \times 2)$ K/Cu(111) system. Our calculations show that the energy level of the quantum-well state is just below E_F , very close to the experimental determination. We also calculate the lifetime broadening of the excited hole in this state whose decay can occur via $e-e$, e -ph, and

electron-defect (e -def) scattering.³³ The latter type of scattering can, in principle, be avoided in scanning tunneling spectroscopy (STS) measurements^{34,35} and strongly reduced in photoemission spectroscopy (PES) study.^{36,37} Therefore, the analysis we present here focuses only on the $e-e$ and e -ph interactions. In the $e-e$ channel, the decay can occur via one-electron energy conserving charge transfer to the bulk states (one-electron scattering) or/and many-body inelastic scattering. The contribution of the former process can be calculated using a wave packet propagation method or local density of states (the spectral function is computed without taking into account the many-body effects).³⁸ The embedding method adopted in this work, thanks to its capability to account for a semi-infinite substrate, is able to accurately describe this term, distinguishing discrete surface states from the resonances that originate from the interaction with the bulk continuum. Here, we show that in contrast to the $p(2 \times 2)$ Na/Cu(111) and Cs/Cu(111) systems, the lifetime broadening of QWS in the $p(2 \times 2)$ K/Cu(111) is mostly determined by many-body $e-e$ scattering and partly by e -ph coupling.

The paper is organized as follows: in Sec. II, we outline the electronic structure calculation method and the model used to evaluate the lifetime broadening. In Sec. III, we report the calculation results and their discussion while in Sec. IV, the conclusions are drawn.

II. THEORY**A. Embedding method**

The calculation of the ground state electronic properties is based on the embedding method developed by Inglesfield,³⁹ within which one is able to consider a localized perturbation in an otherwise perfect infinite substrate. The ground state of the system is accessed through a self-consistent density functional theory (DFT) calculation within a finite region (the

so-called *embedded region*) containing the perturbed volume. In particular, we adopt the implementation of the method proposed by Ishida,^{40,41} for treating realistic surfaces, which assumes the embedded region as being periodically repeated along the x and y directions parallel to the surface, while having a finite extension along the surface normal z . The embedded region in the z direction is chosen large enough to account for the decay of the perturbation and to guarantee a smooth merging of the self-consistent potential with the vacuum one. Along this latter direction, it is bounded by two surfaces where two different nonlocal energy dependent potentials are defined (the embedding potentials); such potentials enter the Kohn-Sham equation acting as boundary conditions reproducing the presence of the two external semi-infinite media. Following the original idea of Nekovee and Inglesfield,^{42,43} it is also possible to exploit the nonperiodicity along the z direction in order to describe the correct asymptotic decay of the image potential, normally not accounted for within DFT.

The geometry of the two-dimensional (2D) unit cell is fixed according to the experimental values, while the extension of the embedded region along the z axis is set to 29 a.u. In this region, we include the two topmost Cu layers and the K one; the remaining vacuum width is about 15 a.u., large enough to account for the slower decay of the states, caused by the work function reduction induced by alkali adsorption.

The Green's function is expanded over a full-potential linearized augmented plane wave (FLAPW) basis set; we chose 10.24 Ry as a cutoff for the plane waves in the interstitial part and $l_{\max}=9$ for the spherical wave expansion inside the Muffin Tins (MTs). The Cu MT radius is $r_{\text{MT}}^{\text{Cu}}=2.40$ a.u., while the K MT one is $r_{\text{MT}}^{\text{K}}=3.25$ a.u.. The surface Brillouin zone (SBZ) was sampled by a 9×9 regular mesh, consisting of 22 independent \mathbf{k}_{\parallel} points. The generalized gradient approximation (GGA) of the exchange and correlation functional as proposed by Burke, Perdew, and Ernzerhof⁴⁴ has been used.

B. Lifetime broadening model

The lifetime broadening Γ ($\Gamma=\Gamma_{e-e}+\Gamma_{e\text{-ph}}=\hbar/\tau$) in paramagnetic metals is determined by $e-e$ scattering and $e\text{-ph}$ interaction. As we show below for the K QWS on Cu(111) the one-electron scattering contribution is small, hence Γ_{e-e} is determined mostly by many-body inelastic $e-e$ scattering. Within many-body theory, the inelastic $e-e$ contribution, Γ_{e-e} , to the lifetime broadening of a hole ($E < E_F$) in a quantum state $\psi(\mathbf{r})$ with energy E is obtained as the projection of the imaginary part of the self-energy $\Sigma(\mathbf{r}, \mathbf{r}'; E)$ onto the state itself

$$\Gamma_{e-e} = 2 \iint d\mathbf{r} d\mathbf{r}' \psi^*(\mathbf{r}) \text{Im} \Sigma(\mathbf{r}, \mathbf{r}'; E) \psi(\mathbf{r}'). \quad (1)$$

The imaginary part of $\Sigma(\mathbf{r}, \mathbf{r}'; E)$ is evaluated by using a *GW* approximation.⁴⁵ Details of such a calculation can be found in Refs. 32 and 46. Wave functions $\psi(\mathbf{r})$ and energies E for 1 ML K/Cu(111) have been evaluated using the one-dimensional potential proposed for alkali metal adlayer on paramagnetic metals.³² Parameters of this potential were de-

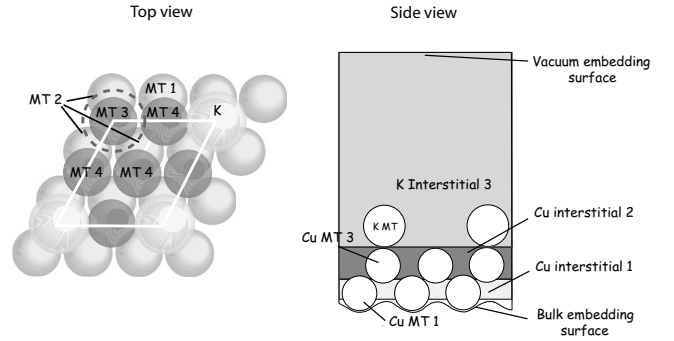


FIG. 1. Sketch of the $p(2 \times 2)\text{K}/\text{Cu}(111)$ unit cell considered in our calculation.

termined by reproducing the energy gap of Cu(111) (Ref. 47) and the experimental energies of QWS (Ref. 30) and the first image state²⁹ of 1 ML K/Cu(111).

We estimate the $e\text{-ph}$ contribution, $\Gamma_{e\text{-ph}}$, to the lifetime broadening by using a Debye model, $\Gamma_{e\text{-ph}}=2\pi\hbar\lambda\omega_D/3$,⁴⁸ where λ and ω_D are the $e\text{-ph}$ coupling strength parameter and Debye frequency, respectively. This model has successfully been used for estimation of $\Gamma_{e\text{-ph}}$ in clean metal surface states^{34,46,49} and in QWSs of metal overlayers on metal substrates,^{32,50} including 1 ML Na/Cu(111).^{32,51}

III. CALCULATION RESULTS AND DISCUSSION

A. Electronic properties

Structural investigations on the K/Cu(111) system were performed experimentally by SEXAFS (Ref. 52) and also theoretically, with different methods.^{53–55} All these studies agree in identifying the equilibrium position of the K atom in the $p(2 \times 2)$ phase as the atop one. The equilibrium distances reported by these investigations are, however, different. The experimental determination is 3.05 ± 0.02 Å while the theoretical ones are in general shorter, and vary according to the method used. Padilla-Campos *et al.*⁵³ studied this system with a cluster model, comparing results obtained within the restricted Hartree-Fock (RHF) approach with those obtained within the DFT in the local density approximation (LDA). The RHF distance is 3.00 Å, being very close to the experimental value, while the DFT one, i.e., 2.90 Å, is slightly shorter. The same authors used this DFT result in order to parametrize a K-Cu interaction potential, which was used in a Metropolis Monte Carlo simulation.⁵⁴ This calculation confirmed the atop adsorption site to be the preferred one at 1 ML coverage ($\theta=0.25$), with the distribution of K-Cu distances centered around 3.00 Å. A further calculation concerning the adsorption configuration of this system has been performed by Doll,⁵⁵ using a slab approach in the DFT framework. These results confirm once again that the atop site is favored, with the K-Cu distance varying from 2.73 Å (LDA) to 2.83 Å (GGA). We choose the SEXAFS data as input configuration for our electronic structure calculation.

We show in Fig. 1 a sketch of the $p(2 \times 2)\text{K}/\text{Cu}(111)$ system in which it is shown how we partition the embedded region into different volumes to which we will refer in the following part of this study. Each 2×2 surface cell contains

TABLE I. Work function in the clean Cu(111) surface and in the K/Cu(111) one.

System	Calculated (eV)	Experimental (eV)
Clean Cu(111)	4.89	4.93 ^b
1 ML K/Cu $p(2 \times 2)$	2.07	2.26 \pm 0.03 ^a

^aReference 29.

^bReference 56.

one K atom and eight Cu ones, four of them are nonequivalent. The total volume is divided into MTs and interstitial regions, which are then further split into three subvolumes, each of which contains the contribution from a single atomic layer (in K interstitial 3 volume also the vacuum region is included). We first analyze the work function change as a consequence of the K adsorption (see data in Table I) obtaining $\phi=4.89$ eV for the clean Cu(111) surface and $\phi=2.07$ eV for the K-covered one. The agreement with experimental data is excellent for what concerns the clean surface while it is slightly worse when the K adlayer is present. Experiments by Fischer *et al.*²⁹ show a small difference (0.2 eV) with our determination, but this discrepancy could be partially ascribed to the fact that the experimental monolayer may have not corresponded to an exact $p(2 \times 2)$ phase.

A general picture of the spectral properties is achieved calculating the density of states (DOS) integrated over the whole SBZ. Fig. 2 reports the DOS pertaining different volumes. Panels (a) and (b) show the DOSs in the subsurface and surface Cu layers, respectively. In the subsurface Cu layer, the DOSs in the two nonequivalent MTs are exactly alike, while there are some differences in the case of the surface layer. The DOS in Cu MT 3 (which is the nearest neighbor of the K atom) is slightly higher than in Cu MT 4 in the energy range between -4 and -3 eV, while there is a

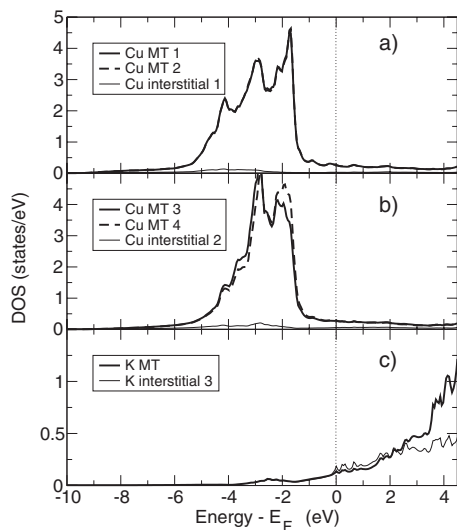


FIG. 2. Layer-projected DOS: (a) subsurface Cu layer, (b) surface Cu layer, and (c) K layer. The thicker lines refer to the DOS integrated in the MT volume, while the thinner ones refer to the interstitial region.

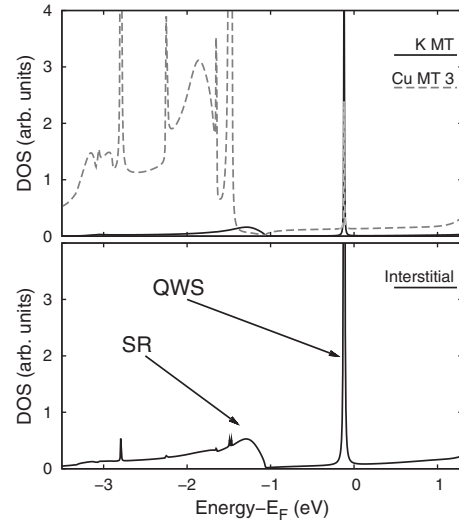


FIG. 3. DOS at $\bar{\Gamma}$ point, evaluated in the surface Cu and in the K layer: (a) MT contributions and (b) interstitial contributions. The peak represents the QWS.

small depletion around -2 eV. Panel (c) of Fig. 2 shows the DOS in the adlayer region. The contributions in the K MT and in the interstitial region are equivalent in the occupied part of the spectrum. This indicates a great delocalization of K valence states at the K/Cu interface.

In order to detect the intrinsic surface features, we consider now the DOS at the fixed value of $\mathbf{k}_{\parallel}=0$, i.e., $\bar{\Gamma}$. Fig. 3 reports the DOS at $\bar{\Gamma}$, evaluated in the surface Cu layer and in the K one. The top panel shows the states in the MTs volumes, while the bottom one shows the interstitial contribution. We note that in the Cu layer the DOS is dominated by the d band (below -1.4 eV), while in the K one, it consists essentially of two features: a broad resonance at about -1.28 eV, which is the surface resonance recently reported by Schiller *et al.*,³⁰ and a sharp peak, whose energy is just below the Fermi level. We identify this peak as the QWS induced by the K adlayer. This state is originated from a two-dimensional charge layer, confined between two potential barriers, which are usually a gap of forbidden bulk states, on the substrate side, and the smooth potential step, on the vacuum side. The presence of such a state in the alkali-covered surfaces has been investigated both theoretically and experimentally^{15,31,32,46} and it is a well known feature of thin and ultrathin metal films on metal substrates.⁵⁰ The QWS plotted in Fig. 3 has a binding energy of -0.118 eV, and it displays a different weight in the volumes considered. The highest contribution is found in the K interstitial 3 volume; the probability density relative to such a state should therefore be higher outside the K atomic volume, reproducing the situation occurring in the Na/Cu(111) system.³¹

In order to further investigate this point, we calculate the distribution of the charge density of the QWS at the $\bar{\Gamma}$ point, as reported in Fig. 4, where the darker (lighter) regions indicate a lower (higher) charge density. The maximum of the charge density is outside the K layer, with a node between the K and the surface Cu layer. This is in agreement with what is expected for a QWS, confirming our assignment. A

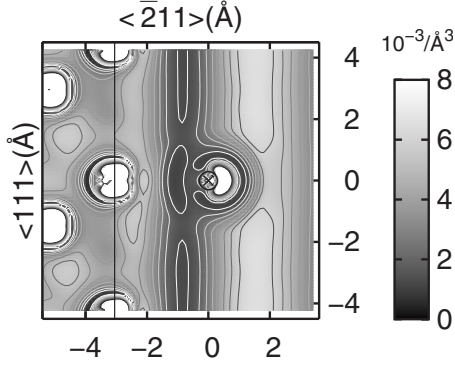


FIG. 4. Charge density distribution relative to the QWS, projected on a plane parallel to the surface normal direction. The higher densities are represented by the lighter regions and the lower densities by the darker ones.

further element arising from Fig. 4 is that this state displays a very small corrugation along the surface plane. We evaluated the dispersion as a function of k_{\parallel} by calculating the DOS along a high-symmetry direction in the SBZ. We chose the $\bar{\Gamma}-\bar{M}$ direction but this should have no influence on the results, since the dispersion of the QWS is isotropic in the SBZ. We display in Fig. 5 such a dispersion, superimposed on the folded continuous bulk bands. The QWS features are summarized in Table II. The effective mass $m^*=0.707 m_e$ is close to the value reported for the Na/Cu(111) case ($0.638m_e$), and it is $\sim 90\%$ of the experimental value. The Fermi wave vector $k_F \sim 0.148 \text{ \AA}^{-1}$ is in very good agreement with the experimental data reported in Ref. 30. It is also in rather good agreement with the value found by Dudde *et al.*,⁵⁷ who report the appearance of this state in inverse photoemission spectroscopy at a value of k_{\parallel} close to 0.2 \AA^{-1} . Given the 2×2 periodicity of the K overlayer, the QWS can interact with the folded part of the surface projected bulk band (lighter gray in Fig. 5). This hybridization is quite small and it gives an elastic width of 2.8 meV. This value is consistent with previously reported data for similar systems, i.e., alkali monolayer on Cu(111).^{28,31,58}

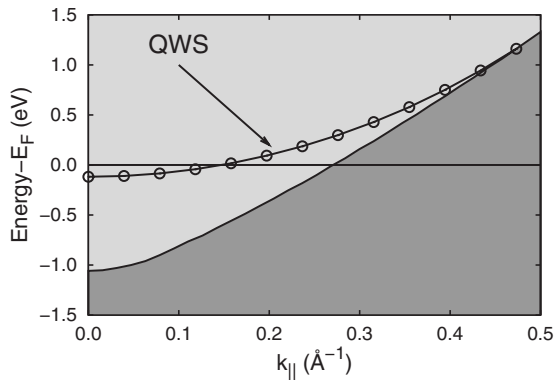


FIG. 5. Dispersion of the QWS along the $\bar{\Gamma}-\bar{M}$ direction. Lighter gray corresponds to the bulk band backfolded in the (2×2) BZ. The continuous line is a guide for the eyes only and does not represent fitting procedure results.

TABLE II. Key features of the QWS of the $p(2 \times 2)$ K/Cu(111). Energies are given with respect to the Fermi level.

	Calculated	Experimental ³⁰
Energy (eV)	-0.118	-0.100
k_F (\AA^{-1})	0.148	~ 0.15
Effective mass (m_e)	0.707	0.81
Γ_{e-ph} (meV)	2	
Γ_{e-e} (meV)	16	
Γ_{elast} (meV)	2.8	

B. Lifetime broadening

As we have shown above, the very sharp QWS resonance at the $\bar{\Gamma}$ point suggests that the dominant contribution in the $e-e$ channel should be the inelastic scattering one. Our calculation for the $\bar{\Gamma}$ QWS gives $\Gamma_{e-e}=16$ meV for $E_{QWS}=-0.11$ eV with an effective mass of the QWS equal to $0.7 m_e$. More than 95% of the 16 meV value originates from intraband transitions within the QWS band itself. The remaining part of Γ_{e-e} comes from interband transitions (transitions bulk states-QW state). Similar mechanism had been found for surface states on the (111) surface of noble metals,^{34,59} on Be(1010), Be(0001),^{46,59} as well as for the $\bar{\Gamma}$ QWS in 1 ML Na/Cu(111).³² Note that in the latter system, the QWS energy is slightly deeper than in $p(2 \times 2)$ K/Cu(111) and therefore one can expect a slightly smaller Γ_{e-e} in $p(2 \times 2)$ K/Cu(111) compared to that in 1 ML Na/Cu(111). However, the calculation of Γ_{e-e} in 1 ML Na/Cu(111) leads to a slightly smaller $\Gamma_{e-e}=13$ meV³² than that in $p(2 \times 2)$ K/Cu(111). This opposite trend can be explained by a slightly higher value for the effective mass of QWS in $p(2 \times 2)$ K/Cu(111).

In order to estimate Γ_{e-ph} , we use the $e-ph$ coupling parameter $\lambda=0.13$ taken for bulk K.⁴⁸ This parameter is not available for QWS in $p(2 \times 2)$ K/Cu(111), however, the calculations of λ in 1 ML Na/Cu(111) (Ref. 51) show that such a value is close to that for the bulk systems. We assume that the same is true for QWS in $p(2 \times 2)$ K/Cu(111). The Debye energy Θ_D used is taken equal to 8 meV.^{60,61} With these parameters, the Debye model gives $\Gamma_{e-ph}=2$ meV, which is significantly smaller than the $e-e$ contribution. This value is also essentially smaller than $\Gamma_{e-ph}=8.5$ meV³² for the 1 ML Na/Cu(111) system that can be explained by bigger values of Θ_D and λ used for such a system.

The obtained data clearly indicate that the lifetime broadening of the $\bar{\Gamma}$ QWS in $p(2 \times 2)$ K/Cu(111) is not negligible and is essentially determined by many-body $e-e$ interaction. One-electron scattering and $e-ph$ interaction contributions are quite small. This physical picture is completely different from that for $p(2 \times 2)$ Na/Cu(111) and $p(2 \times 2)$ Cs/Cu(111) where the $e-e$ inelastic (many-body) contribution is very small and the total Γ is determined by one-electron scattering and $e-ph$ contributions.²⁸

IV. CONCLUSIONS

In this study, we presented a characterization of the electronic properties of the QWS in the $p(2 \times 2)$ K/Cu(111) sys-

tem, which was the subject of some experimental investigations, in which particular attention has been devoted to the investigation of the QWS features.^{29,30}

The theoretical method we adopted takes advantage of the extended metal substrate to well account for the interaction between the overlayer localized states and the continuum of the metal band. The energy and dispersion of the QWS we calculate indeed agree well with the experimental data.

We also considered the linewidth of the QWS, which is determined by different decay mechanisms. The $e-e$ elastic width contribution is due to the resonant tunneling between the QWS and the surface projected bulk band and has been quantified as being 2.8 meV. The other $e-e$ contributions,

due to interband and intraband transitions, are many-body effects that we considered within the GW approximation. According to our calculation, their contribution to the total width is 16 meV and it is dominated by the intraband transitions within the QWS band itself. We also evaluated the impact of the electron-phonon interaction on the linewidth within the Debye model obtaining a value of 2 meV.

In contrast with other alkali adlayers on Cu(111), in the K/Cu(111) system the QWS linewidth is mainly determined by many-body electron-electron interaction. The analysis done in the paper can be useful for the interpretation of the electron excitation dynamics occurring within alkali overlayers on other metal substrates.

-
- ¹R. W. Gurney, *Phys. Rev.* **47**, 479 (1935).
²M. Bauer, S. Pawlik, and M. Aeschlimann, *Phys. Rev. B* **55**, 10040 (1997).
³M. Bauer, S. Pawlik, and M. Aeschlimann, *Phys. Rev. B* **60**, 5016 (1999).
⁴S. Ogawa, H. Nagano, and H. Petek, *Phys. Rev. Lett.* **82**, 1931 (1999).
⁵H. Petek, H. Nagano, M. J. Weida, and S. Ogawa, *Science* **288**, 1402 (2000).
⁶J. Zhao *et al.*, *Phys. Rev. B* **78**, 085419 (2008).
⁷J. W. Gadzuk, *Surf. Sci.* **6**, 133 (1967).
⁸N. D. Lang and A. R. Williams, *Phys. Rev. B* **18**, 616 (1978).
⁹J. P. Muscat and D. M. Newns, *Prog. Surf. Sci.* **9**, 1 (1978).
¹⁰H. Ishida, *Phys. Rev. B* **38**, 8006 (1988).
¹¹P. Nordlander and J. C. Tully, *Phys. Rev. B* **42**, 5564 (1990).
¹²A. G. Borisov, J. P. Gauyacq, A. K. Kazansky, E. V. Chulkov, V. M. Silkin, and P. M. Echenique, *Phys. Rev. Lett.* **86**, 488 (2001).
¹³A. G. Borisov, J. P. Gauyacq, E. V. Chulkov, V. M. Silkin, and P. M. Echenique, *Phys. Rev. B* **65**, 235434 (2002).
¹⁴J. P. Gauyacq, A. G. Borisov, and M. Bauer, *Prog. Surf. Sci.* **82**, 244 (2007).
¹⁵J. Kliewer and R. Berndt, *Phys. Rev. B* **65**, 035412 (2001).
¹⁶D. Heskett, K.-H. Frank, E. E. Koch, and H.-J. Freund, *Phys. Rev. B* **36**, 1276 (1987).
¹⁷G. A. Benesh and J. R. Hester, *Surf. Sci.* **194**, 567 (1988).
¹⁸S. Å. Lindgren and L. Walldén, *Phys. Rev. B* **38**, 3060 (1988).
¹⁹E. V. Chulkov and V. M. Silkin, *Surf. Sci.* **215**, 385 (1989).
²⁰N. Fischer, S. Schuppler, R. Fischer, Th. Fauster, and W. Steinmann, *Phys. Rev. B* **43**, 14722 (1991).
²¹R. Fasel, P. Aebi, R. G. Agostino, L. Schapbach, and J. Osterwalder, *Phys. Rev. B* **54**, 5893 (1996).
²²A. Carlsson, B. Hellsing, S. Å. Lindgren, and L. Walldén, *Phys. Rev. B* **56**, 1593 (1997).
²³C. Stampfl, K. Kambe, R. Fasel, P. Aebi, and M. Scheffler, *Phys. Rev. B* **57**, 15251 (1998).
²⁴J. M. Carlsson and B. Hellsing, *Phys. Rev. B* **61**, 13973 (2000).
²⁵T.-C. Chiang, *Surf. Sci. Rep.* **39**, 181 (2000).
²⁶A. K. Kazansky, A. G. Borisov, and J. P. Gauyacq, *Surf. Sci.* **544**, 309 (2003).
²⁷J. Algdal, T. Balasubramanian, M. Breitholtz, V. Chis, B. Hellsing, S. Å. Lindgren, and L. Walldén, *Phys. Rev. B* **78**, 085102 (2008).
²⁸C. Corriol, V. M. Silkin, D. Sánchez-Portal, A. Arnau, E. V. Chulkov, P. M. Echenique, T. von Hofe, J. Kliewer, J. Kröger, and R. Berndt, *Phys. Rev. Lett.* **95**, 176802 (2005).
²⁹N. Fischer, S. Schuppler, R. Fischer, Th. Fauster, and W. Steinmann, *Phys. Rev. B* **47**, 4705 (1993).
³⁰F. Schiller, M. Corso, M. Urdanpilleta, T. Ohta, A. Bostwick, J. L. McChesney, E. Rotenberg, and J. E. Ortega, *Phys. Rev. B* **77**, 153410 (2008).
³¹G. Butti, S. Caravati, G. P. Brivio, M. I. Trioni, and H. Ishida, *Phys. Rev. B* **72**, 125402 (2005).
³²E. V. Chulkov, J. Kliewer, R. Berndt, V. M. Silkin, B. Hellsing, S. Crampin, and P. M. Echenique, *Phys. Rev. B* **68**, 195422 (2003).
³³E. V. Chulkov, A. G. Borisov, J. P. Gauyacq, D. Sánchez-Portal, V. M. Silkin, V. P. Zhukov, and P. M. Echenique, *Chem. Rev. (Washington, D.C.)* **106**, 4160 (2006).
³⁴J. Kliewer, R. Berndt, E. V. Chulkov, V. M. Silkin, P. M. Echenique, and S. Crampin, *Science* **288**, 1399 (2000).
³⁵J. Kröger, L. Limot, H. Jensen, R. Berndt, S. Crampin, and E. Pehlke, *Prog. Surf. Sci.* **80**, 26 (2005).
³⁶F. Reinert, G. Nicolay, S. Schmidt, D. Ehm, and S. Hüfner, *Phys. Rev. B* **63**, 115415 (2001).
³⁷F. Reinert, *J. Phys.: Condens. Matter* **15**, S693 (2003).
³⁸For discussion of these details, see Ref. 33 and references therein.
³⁹J. E. Inglesfield, *J. Phys. C* **14**, 3795 (1981).
⁴⁰H. Ishida, *Surf. Sci.* **388**, 71 (1997).
⁴¹H. Ishida, *Phys. Rev. B* **63**, 165409 (2001).
⁴²M. Nekovee and J. E. Inglesfield, *EPL* **19**, 535 (1992).
⁴³M. Nekovee and J. E. Inglesfield, *Prog. Surf. Sci.* **50**, 149 (1995).
⁴⁴J. P. Perdew, K. Burke, and M. Ernzerhof, *Phys. Rev. Lett.* **77**, 3865 (1996).
⁴⁵L. Hedin and S. Lundqvist, *Solid State Phys.* **23**, 1 (1970).
⁴⁶P. M. Echenique, P. Berndt, E. V. Chulkov, Th. Fauster, A. Goldmann, and U. Höfer, *Surf. Sci. Rep.* **52**, 219 (2004).
⁴⁷E. V. Chulkov, V. M. Silkin, and P. M. Echenique, *Surf. Sci.* **437**, 330 (1999).
⁴⁸G. Grimvall, *The Electron-Phonon Interaction in Metals* (North-Holland, Amsterdam, 1981).
⁴⁹B. A. McDougall, T. Balasubramanian, and E. Jensen, *Phys. Rev.*

- B **51**, 13891 (1995).
- ⁵⁰M. Milun, P. Pervan, and D. P. Woodruff, *Rep. Prog. Phys.* **65**, 99 (2002).
- ⁵¹S. V. Eremeev, I. Sklyadneva, P. M. Echenique, S. D. Borisova, G. Benedek, G. G. Rusina, and E. V. Chulkov, *Surf. Sci.* **601**, 4553 (2007).
- ⁵²D. L. Adler *et al.*, *Phys. Rev. B* **48**, 17445 (1993).
- ⁵³L. Padilla-Campos, A. Toro-Labbé, and J. Maruani, *Surf. Sci.* **385**, 24 (1997).
- ⁵⁴L. Padilla-Campos and A. Toro-Labbé, *J. Chem. Phys.* **108**, 6458 (1998).
- ⁵⁵K. Doll, *Eur. Phys. J. B* **22**, 389 (2001).
- ⁵⁶W. Wallauer and Th. Fauster, *Surf. Sci.* **374**, 44 (1997).
- ⁵⁷R. Dudde, K. H. Frank, and B. Reihl, *Phys. Rev. B* **41**, 4897 (1990).
- ⁵⁸V. Chis, S. Caravati, G. Butti, M. I. Trioni, P. Cabrera-Sanfeliu, A. Arnau, and B. Hellsing, *Phys. Rev. B* **76**, 153404 (2007).
- ⁵⁹E. V. Chulkov, V. M. Silkin, and M. Machado, *Surf. Sci.* **482-485**, 693 (2001).
- ⁶⁰C. Kittel, *Introduction to Solid State Physics* (Wiley, New York, 1995).
- ⁶¹N. W. Ashcroft and D. N. Mermin, *Solid State Physics* (Thomson Learning, Toronto, 1976).